New Phytologist

# Exploration of the late stages of the tomato–*Phytophthora parasitica* interactions through histological analysis and generation of expressed sequence tags

Jo-Yanne Le Berre, Gilbert Engler and Franck Panabières

UMR INRA1064/CNRS 6192/UNSA Interactions Plantes – Microorganismes et Santé Végétale, Centre INRA de Sophia-Antipolis, BP 167, 400 route des Chappes, 06903 Sophia-Antipolis Cedex, France

Author for correspondence:
*F. Panabières*
*Tel: +33 4 92 38 65 18*
*Fax: +33 4 92 38 65 87*
*Email: panab@antibes.inra.fr*

Received: *2 July 2007*
Accepted: *24 August 2007*

## Summary

• The oomycete *Phytophthora parasitica* is a soilborne pathogen infecting numerous plants. The infection process includes an initial biotrophic stage, followed by a necrotrophic stage. The aim here was to identify genes that are involved in the late stages of infection.

• Using the host tomato and a transformed strain of *P. parasitica* expressing the green fluorescent protein (GFP), the various infection steps from recognition of the host to the colonization of plant tissues were studied. This late stage was selected to generate 4000 ESTs (expressed sequence tags), among which approx. 80% were from the pathogen.

• Comparison with an EST data set created previously from *in vitro* growth of *P. parasitica* allowed the identification of several genes, the expression of which might be regulated during late stages of infection.

• Changes in gene expression of several candidate genes predicted from *in silico* analysis were validated by quantitative RT–PCR experiments. These results give insights into the molecular bases of the necrotrophic stage of an oomycete pathogen.

**Key words:** confocal microscopy, expressed sequence tags (ESTs), green fluorescent protein (GFP), interaction, *Phytophthora*, transformation.

*New Phytologist* (2008) **177**: 480–492

**doi**: 10.1111/j.1469-8137.2007.02269.x



## Introduction

*Phytophthora* plant pathogens cause the majority of devastating diseases of cultivated crops and land communities worldwide (Erwin & Ribeiro, 1996). Nearly all species are considered plant pathogens, but they differ in their lifestyles, host range and infection mode. For example, *Phytophthora infestans* (the potato late blight pathogen) and *Phytophthora sojae* (soybean root rot pathogen) infect few plants, while *P. parasitica* (= *P. nicotianae*) attacks up to 60 plant families. *Phytophthora infestans* is an airborne, foliar pathogen, while most species, including *P. sojae* and *P. parasitica*, are soilborne root and stem pathogens (Erwin & Ribeiro, 1996).

*Phytophthora* species are considered hemibiotrophs, because they maintain biotrophic relationships with their host for part of their life cycle. Invasion by root pathogens begins through intercellular penetration between root epidermal cells (Benhamou & Côté, 1992), followed by both intra- and intercellular growth, and severe disruption of plant cells is observed even at early steps of invasion, suggesting that the biotrophic stage is rather short, if really observable (Hanchey & Wheeler, 1971).

To gain insight into the molecular mechanisms underlying the *Phytophthora*–plant interactions and improve pest management strategies, researchers have developed genomic tools for a few species. To date, the complete genomes of *P. sojae* and *Phytophthora ramorum*, the sudden oak death agent, have been described (Tyler *et al.*, 2006). The *P. infestans* genome is now publicly available on the website of the Broad Institute (http://www.broad.mit.edu/annotation/genome/

phytophthora_infestans/Home.html), and the sequencing of other genomes is ongoing. Meanwhile, the *Phytophthora* transcriptomes have been investigated before or during the early phases of infection. Studies were conducted on zoospores, germinated cysts and appressoria, favouring differential approaches, and leading to the identification of genes regulated during early stages of infection (Pieterse *et al.*, 1993; Beyer *et al.*, 2002; Avrova *et al.*, 2003; Shan *et al.*, 2004b; Skalamera *et al.*, 2004:; Grenville-Briggs *et al.*, 2005). However, few reports describe genes expressed during later stages, such as colonization and necrotrophy (Qutob *et al.*, 2002; Moy *et al.*, 2004; Torto-Alalibo *et al.*, 2007), which cause the most important damage to plants under field conditions. *Phytophthora infestans* and *P. ramorum* are not suitable for such studies because of the low biomass of pathogen in infected tissues (*P. infestans*) or to the technical limitations encountered on woody hosts (*P. ramorum*). In addition, published reports about large-scale identification of *Phytophthora* genes expressed during interaction concern *c.* 700 ESTs derived from soybean hypocotyls artificially infected by *P. sojae* (Qutob *et al.*, 2000) and *c.* 970 ESTs from mixed *P. infestans*/plant libraries (Randall *et al.*, 2005).

As a root pathogen, and because of its broad host range, *P. parasitica* is representative of many *Phytophthora* species. Consequently data obtained on interactions between this pathogen and its hosts would be easily transposable to other species. We intended to identify the mechanisms underlying pathogenicity in the late phases of tomato infection by *P. parasitica*. Generating a collection of ESTs from infected tissues would permit us to reach this goal. This paper deals with a combination of histological and molecular approaches. We generated a transformed *P. parasitica* strain expressing the green fluorescent protein (GFP) as a vital marker, in order to explore the plant infection at high resolution under *in vivo* conditions. This allowed the time course of infection to be monitored using confocal laser scanning microscopy, to ensure the pathogen entered its necrotrophic stage. The second part of this work describes the generation of *c.* 4000 ESTs derived from infection, their annotation in the context of histological observations, and their comparison with an EST data set derived from *P. parasitica* mycelium grown *in vitro* (Panabières *et al.*, 2005). This work raises several hypotheses concerning the global changes in gene expression during host colonization, and constitutes a first step towards dissecting the molecular events controlling the establishment of necrotrophy in *Phytophthora*.

## Materials and Methods

### Oomycete and plant material

*Phytophthora parasitica* Dastur isolate 149 was isolated from tomato, preserved in liquid nitrogen and routinely cultured on malt agar at 24°C. Tomato plantlets (*Lycopersicon esculentum* Mill. cv. Microtom) (Meissner *et al.*, 1997) were grown for 3 wk after the onset of germination on a modified agar medium derived from Murashige and Skoog (Colas *et al.*, 1998), transferred to plastic bridges on the same medium without agar (in 5 ml final volume), and rooted for an additional 3 wk until inoculation with *P. parasitica*.

### Transformation of *P. parasitica*

The transformation vector pTefGHNH harbours two cassettes in a tail-to-head orientation (Fig. S1 in Supplementary Material). Each cassette was derived from the vector pTH209 (Judelson, 1993) and possessed either the *nptII* gene conferring resistance to geneticin (G418) or the coding sequence of the GFP located in an *Nco*I–*Kpn*I fragment of the plasmid pEGFP-C1 (Clontech, Palo Alto, CA, USA), upstream from the *Bremia lactucae Ham34* terminator (Judelson, 1993). The *Hsp70* promoter of pTH209 was replaced by the promoter of *P. parasitica* translation elongation factor 1 (*PpTef1*), designed as *PpTef1Prom*. *PpTef1* was selected because it appeared to be constitutively expressed in *P. parasitica* (J.-Y.L.B. and F.P., unpublished results). The full-length *PpTef1* cDNA was obtained by assembling *P. parasitica* ESTs (Panabières *et al.*, 2005; accession number DQ138080). *PpTef1prom* consisted of an 1181-bp fragment upstream from the *PpTef1* start codon that was obtained by inverse PCR. Protoplasts from *P. parasitica* were prepared as described (Bottin *et al.*, 1999). Transformation was achieved according to published protocols (Judelson, 1993; Bottin *et al.*, 1999) using $10^8$ protoplasts and 30 μg DNA. Selection was performed in the presence of 5 μg $ml^{-1}$ G418 for 3 d. Plates were overlaid with V8 agar containing 10 μg $ml^{-1}$ G418. After an additional 3 d, they were overlaid with V8 agar medium containing 20 μg $ml^{-1}$ G418. Following single-spore isolation, G418-resistant transformants were propagated on V8 medium containing 20 μg $ml^{-1}$ G418 at 24°C.

### Biological assays

For inoculation, the modified MS medium was removed and replaced by sterile water before adding 25 μl of a solution containing 500 zoospores. The plants were kept at 24°C with 16 h daily illumination, and were observed daily. Pathogen invasion was monitored by confocal laser scanning microscopy (CLSM); infected root samples were mounted in water, covered with a cover slip and immediately observed with a Zeiss LSM 510 META confocal microscope (Carl Zeiss Jena GmbH, Jena, Germany). The 488-nm line of an Argon laser in combination with the 543-nm line of an HeNe laser were used in a Multi Track scan configuration to image hyphal GFP and plant cell wall autofluorescence. The two signals were differentiated via emission windows: 505–530 nm for GFP (green) and 560 nm for autofluorescence (red). To observe cell disintegration, propidium iodide was added to a final concentration of 5 μg $ml^{-1}$.

 

### RNA isolation, cDNA and library construction

RNA extraction from vegetative cultures was performed as described previously (Panabières *et al.*, 2005). Total RNA from freeze-dried infected roots was isolated according to (Laroche-Raynal *et al.*, 1984). Poly(A)$^+$ RNA purification and construction of the unidirectional cDNA library were conducted as described previously (Panabières *et al.*, 2005). The titre of the library before amplification was 800 000 cfu. After mass excision and plating, individual colonies were picked arbitrarily and transferred to 42 96-well microtitre plates for sequencing, in order to generate 4032 ESTs. Plasmid DNA miniprep and sequencing were performed by Genome Express SA (Meylan, France).

### Expression pattern analyses, real time RT–PCR assays and statistics

Candidate genes were selected on the basis of differential representation between the two EST libraries. The likelihood of differential expression of these genes was calculated according to methods described by Audic & Claverie (1997) for same-size, nonnormalized libraries, using the web interface hosted at the Information Génomique et Structurale server (http://www.igs.cnrs-mrs.fr/SpipInternet). A significant differential expression was presumed if $P < 0.05$.

For experimental validation, primer pairs (see Table 3) were designed using PRIMER3 (http://frodo.wi.mit.edu). The amplification efficiency of all primer pairs was evaluated with *P. parasitica* genomic DNA as a template. After reactions, samples were electrophoresed on agarose gels to verify amplification of the target fragments. The gene encoding ubiquitin-conjugating enzyme (Ubc) was selected as constitutively expressed internal control (Yan & Liou, 2006). All assays were carried out in triplicate. First-strand cDNAs were synthesized from 1 μg total RNA in a 20-μl reaction using the i-script cDNA synthesis kit (Bio-Rad, Hercules, CA, USA) according to the manufacturer's instructions. cDNA was diluted 50-fold, and quantitative real-time PCR experiments were performed using 5 μl cDNA in a 15-μl final volume using absolute SyberGreen (Eurogentec SA, Seraing, Belgium) oligonucleotides at a 130 nM final concentration. The quantification of gene expression was performed using the relative quantification ($\Delta\Delta C_T$) method, and comparing the data with the internal control, expression of which was determined to remain constant in the different RNA preparations.

### Sequence processing and analysis

Raw sequences were processed manually, assembled into contigs and annotated as described (Panabières *et al.*, 2005). All unisequences have been deposited in GenBank (accessions EC912118 to EC915232). Similarities were searched against the GenBank nonredundant protein database (nr) using BLASTX, and against the dbEST database using BLASTN. Sequences were also compared with all *P. parasitica* ESTs available (Shan *et al.*, 2004b; Skalamera *et al.*, 2004; Panabières *et al.*, 2005) installed on a local database using BIOEDIT, with ESTs from *P. sojae* located at the Virginia microbial database (Tripathy *et al.*, 2006), ESTs from *P. infestans* deposited in GenBank, with the *P. ramorum* and *P. sojae* draft genomes (Tyler *et al.*, 2006) deposited at the Joint Genome Institute, Department of Energy (http://genome.jgi-psf.org) and with the first assembly of the *P. infestans* genome available at the Broad Institute server (www.broad.mit.edu). Similarities were also searched against the tomato, pepper and potato sequences deposited at the TIGR site (http://compbio.dfci.harvard.edu/tgi/cgi-bin/tgi/Blast/index.cgi). Annotation included searches against the Interpro (Apweiler *et al.*, 2001), COGEME (Soanes *et al.*, 2002) and MEROPS peptidase (Rawlings & Barrett, 1999) databases. Signal peptides and subcellular localization were predicted using the SIGNALP and TARGETP servers of the Center for Biological Sequence (http://www.cbs.dtu.dk) and the PSORT II algorithm (Nakai & Kanehisa, 1992) (http://psort.ims.u-tokyo.ac.jp).

## Results and Discussion

### Transformation of *P. parasitica*

The coding sequence of the GFP gene was introduced into *P. parasitica* 149, a strain highly aggressive on tomato, by the protoplast transformation method (Judelson, 1993), along with a selection marker (*nptII*, conferring resistance to G418). Numerous colonies grew on the selective medium but showed a marked reduction in fitness compared with untransformed controls, and were considered as false positives. Two G418$^R$ transformants exhibiting an unaffected growth rate were selected for further experiments. They both contained a single copy of the transgene, as verified by Southern blot hybridizations (not shown). Zoospore preparations were plated on G418-amended medium over four rounds of single-zoospore isolation, to ensure that transformation was stable. One transformant showed an intense fluorescence that was readily visible, even under the binocular microscope at low magnification (not shown), and was chosen for use in biological assays.

### Monitoring plant infection by *P. parasitica*

Tomato infection was performed by adding a moderate amount of inoculum (500 zoospores) to unwounded roots. This system had already been used to evaluate the diversity of virulence of *P. parasitica* on tobacco (Colas *et al.*, 1998). Uninfected tomato roots produced a red autofluorescent signal that did not interfere with the fluorescence of GFP (Fig. 1b). At 1 d after adding zoospores, plantlets appeared healthy, and only few hyphae developed on or around the roots. By contrast, microscopic analysis revealed that the

 

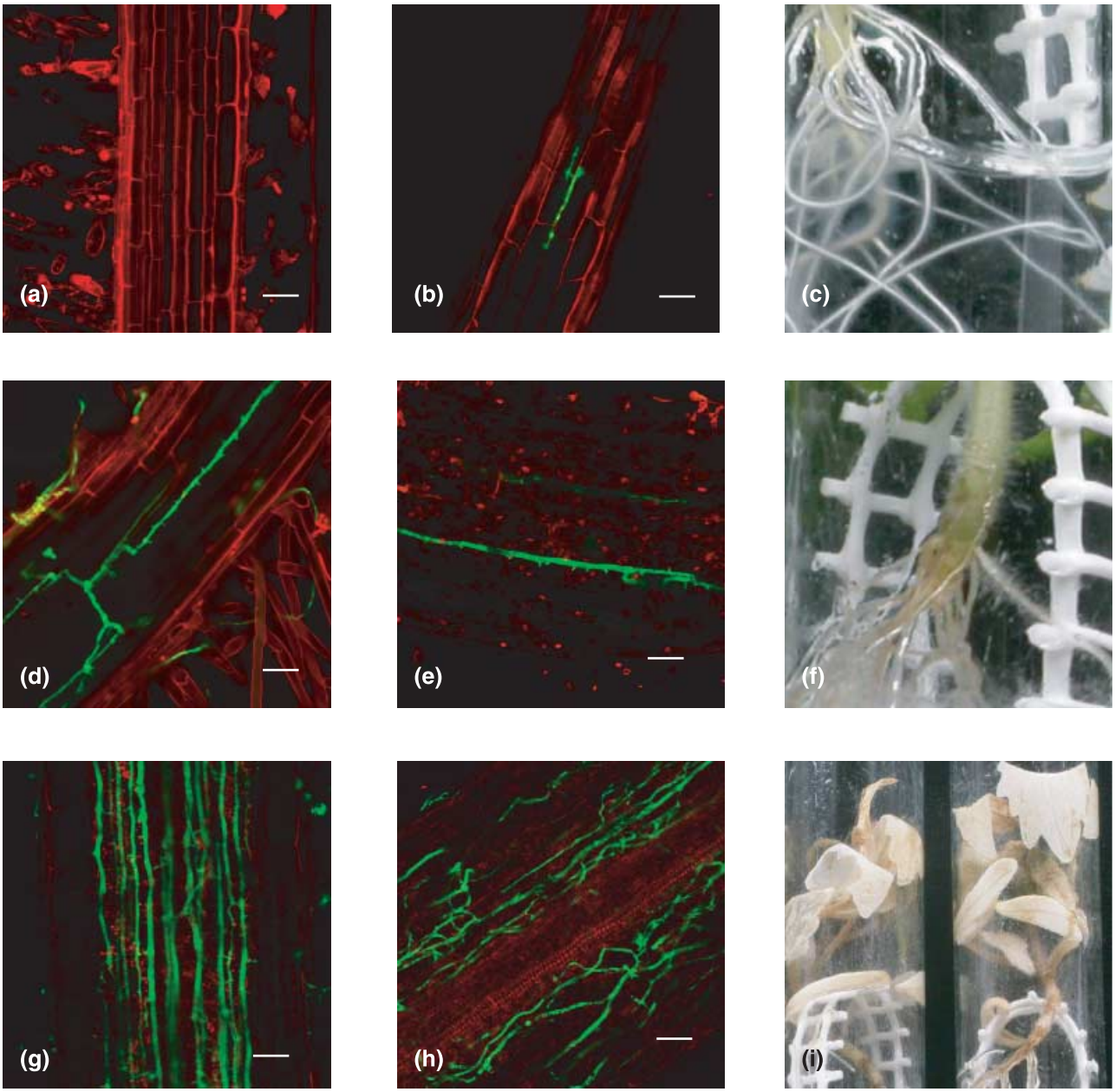


**Fig. 1** Infection of 6-wk tomato plantlets by *Phytophthora parasitica*. Both macroscopic confocal laser scanning microscopic analyses are presented. (a) Inner observation of uninfected roots using propidium iodine. Cell walls are intact and nuclei are not visible. (b) *P. parasitica* hyphae in contact with the tomato root surface. (c) Macroscopic observation of hyphal development after 2 d. (d) Microscopic observation revealing mycelial growth inside the tomato root 2 d after inoculation (dpi). (e) 'Barbed wire'-like structures formed by expanding hyphae in contact with tomato cells. (f) Wilting symptoms at the collar 4 d after inoculation. (g) Colonization of root tissues by *P. parasitica* 4 dpi. (h) The central cylinder and xylem vessels remain intact. Bar, 50 μm. (i) Symptoms observed 10 dpi.

pathogen was already present in host tissues (Fig. 1b). At 2 d post-inoculation (dpi), plants were healthy as observed macroscopically, but mycelium had developed within the root hairs (Fig. 1c). Microscopic exploration revealed that the pathogen invaded plant tissues (Fig. 1d). No haustoria were observed, but small hooks were frequently visible, suggesting that entry into host cells had occurred, giving the hyphae a 'barbed wire'-like appearance (Fig. 1e). These structures were also observed during vegetative growth *in vitro*, ruling out the hypothesis that they may constitute genuine haustoria (not shown). Using propidium iodide allowed extensive staining of cellular components, indicating that cell walls have been destroyed, and that *P. parasitica* had already entered its necrotrophic stage at this time, despite the lack of external symptoms. After 3 d, plants did not display any disease symptoms macroscopically, although microscopic observation

 

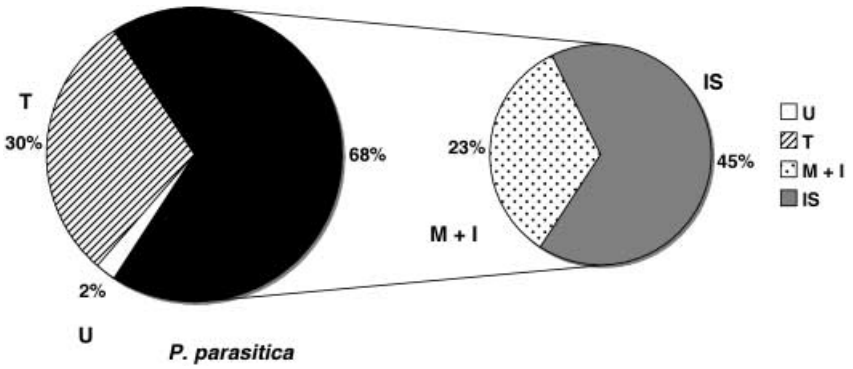


**Fig. 2** Characterization of the *Phytophthora parasitica* ESTs and origin of sequences within the interaction library contig set. IS, Interaction-specific sequences; M + I, contigs present in the mycelium library (Panabières *et al*., 2005); T, tomato sequences; U, sequences unclassified.

indicated that hyphal growth was significant. At 4 dpi, wilting symptoms appeared at the collar (Fig. 1f) and roots were totally engulfed by mycelium. The root tissues were extensively overgrown (Fig. 1g), with the exception of the xylem vessels that evaded invasion (Fig. 1h). After this date, severe damage occurred rapidly to the aerial parts until plant death, which frequently occurred after a 10-d period (Fig. 1i). Monitoring infection microscopically was very difficult beyond 4 d because the tomato tissues showed loss of firmness, hampering manipulation. Given the large pathogen biomass accumulating after 4 d, this stage was chosen to construct the cDNA library in order to obtain an overview of genes expressed during the necrotrophic stage of infection. However, the timing of infection could have been altered by use of the GFP transformant, differing from that expected with a wild-type strain. So the untransformed strain 149 was used to infect tomato plantlets under conditions similar to those carried out with the GFP strain. No differences were observed on the timing or extent of symptoms, so we constructed the cDNA library from roots infected with the wild-type strain to avoid any putative effect of transgene integration on the *P. parasitica* transcriptome.

## Characterization of the EST collection

We sequenced 4032 clones; after removal of clones without inserts, low-quality reads and contaminating mitochondrial or rRNA sequences, 3908 ESTs remained. Following assembly, 2475 cDNAs were identified, consisting of 546 contigs of two to 57 ESTs, 1929 singletons. The overall redundancy (Panabières *et al*., 2005) was estimated at 50.6%. Up to 11% of total ESTs (429/3908) were assembled into 24 genes (0.97% of total unisequences) while 97% of unique sequences (2403/2475) were represented by only one to five ESTs. As the library included transcripts from both infected plant tissues and invading hyphae, the sequences were compared with oomycete genomes and data from solanaceae. ESTs without obvious similarity to any organism were further scrutinized for their G + C content, which is on average higher for *Phytophthora* than for plants (Qutob *et al*., 2000; Huitema *et al*., 2003). Among these, 55 unigenes (57 ESTs) displayed a G + C content of 50%, and were discarded from the analysis. Tomato sequences represented 23.6% (862/3851) of the EST set and were assembled into 731 cDNAs. The remaining ESTs were ascribed to *P. parasitica* and constituted 1689 unigenes. Among the *P. parasitica* sequences (designed as an 'interaction library'), 567 unigenes were also present in ESTs generated from vegetative growth (designed as a 'mycelium library', Panabières *et al*., 2005). So the present work allowed the identification of 1122 novel *P. parasitica* cDNAs, representing approx. 45% of the contig set (Fig. 2; Table S1). Grouping of sequences into functional categories was carried out using the MIPS classification, including the small modifications already described (Panabières *et al*., 2005), leaving 542 unisequences (23.9%) in an 'unknown' category. This functional classification followed gene identification based on BLAST searches. However, caution had to be exercised in some cases when BLAST similarity values were particularly low (e-04 or lower).

To determine sequence conservation within *Phytophthora*, and to identify sequences potentially specific to *P. parasitica*, we used BLASTN and BLASTX to search the genomes of *P. infestans*, *P. ramorum* and *P. sojae*. Starting with an *E* value cutoff of $10^{-10}$, 147 unisequences (152 ESTs) gave no significant hits in any genome, and might be specific to *P. parasitica*. Most of these (91.2%) did not match to proteins from nonredundant databases. However, two of these genes would encode proteins possessing a signal peptide for secretion and an RxLRdEER motif near the N-terminus. This motif has been identified in a number of potential effectors (Kamoun, 2006), including the avirulence genes *Avrb1* from *P. sojae* (Shan *et al*., 2004a), *Avr3a* of *P. infestans* (Armstrong *et al*., 2005) and *Atr1* and *Atr13* of *Hyaloperonospora parasitica* (Rehmany *et al*., 2005), and is proposed to participate in transporting effectors into the plant cytoplasm. Four genes contained a domain for protein kinase, and a contig of seven ESTs displayed similarities to a serine palmitoyl CoA transferase. It was also found in the mycelium library, confirming that it is actually a *Phytophthora* sequence. In addition, 34 unisequences gave very weak similarities to the three *Phytophthora* genomes, and 193 genes (258 ESTs) failed to match with one or two genomes (Fig. 3). These frequently consisted of unknown or hypothetical proteins, but noticeable exceptions were glutamine synthase, phosphoglycerate kinase, and a set of several potential

 

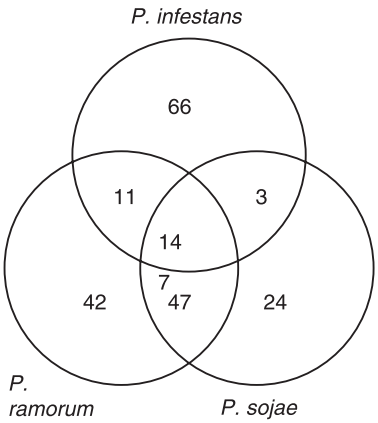


**Fig. 3** Venn diagram displaying the number of *Phytophthora parasitica* unisequences without homologues in one or several *Phytophthora* genomes.

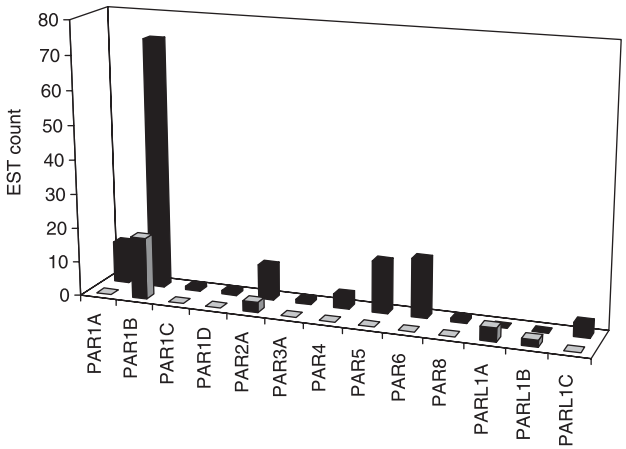


**Fig. 4** Distribution of elicitin and elicitin-like sequences determined by comparative EST representation (mycelium library 3568, closed bars; interaction library 2989, open bars). Nomenclature adapted from Jiang *et al*. (2006).

ribosomal proteins that diverged strongly from the *P. infestans* genes, a potential phospholipid hydroperoxide glutathione peroxidase and a gene possessing a ubiquitin domain that did not match to the *P. ramorum* genome, and a putative ubiquitin ligase that did not match to the *P. sojae* proteome. Setting an $E$ value cutoff to $10^{-2}$ did not give significantly different results.

## Identification of effectors and proteins involved in the secretion process

We looked for the various families of effectors that are proposed, or have been shown, to trigger or manipulate host cell defences. These have recently been classified as apoplastic or cytoplasmic effectors, according to their potential targeting site in the host plant (Kamoun, 2006). Among potential apoplastic effectors, we found two small cysteine-rich (SCR) proteins exhibiting significant similarity to the *P. infestans* SCR108 and SCR122 proteins, respectively (Torto *et al*., 2003), and two members of the widely distributed Nep-like proteins (Gijzen & Nurnberger, 2006), although divergence was too large to identify orthologues properly. Two cDNAs displayed extensive or moderate similarity with transglutaminase M81, respectively (85% identity at the nucleotide level over 800 bp, $E$ = e-102; 74% identity over 250 bp, $E$ = 3e-25). This enzyme belongs to a family of elicitors initially identified in *P. sojae* as a 42-kDa glycoprotein, containing a 13-residue domain required for transglutaminase as well as elicitor activities (Brunner *et al*., 2002). In *P. infestans*, members of this family appear to display divergent stage-specific patterns of expression, although the infection stages have not been explored (Fabritius & Judelson, 2003). Three cDNAs showed similarity to CBEL, originally described in *P. parasitica* (Villalba Mateos *et al*., 1997). This 34-kDa glycoprotein possesses two regions with similarity to the PAN module (Interpro, IPR000177) and may be involved in cell wall deposition in *P. parasitica* (Gaulin *et al*., 2002). One cDNA was identical to the sequence originally published, while another diverged only by a T–C transition in the signal peptide region, and a 10-aa deletion in the Thr/Pro rich spacer in one sequence, shortening the distance between the cellulose-binding domains. The third cDNA showed only weak similarity (41% positive, $E$ = 3e-08) to CBEL, essentially centred on the PAN domain, and may correspond to a distinct class of genes.

Among apoplastic effectors, the elicitin superfamily was represented by 27 ESTs, assembled into four cDNAs. The most abundant, PARA1 (Colas *et al*., 2001), was assembled from 18 ESTs, while a contig of three ESTs encoded the 174-aa elicitin-like PAR2A (Panabières *et al*., 2005). Two contigs of four and two ESTs encoded elicitin-like proteins (ELL) of 187 and 253 aa, including the 20-aa signal peptide, named PAR9 and PAR10, respectively. They contained six cysteine residues and a core domain of 85 amino acids, instead of 98 as observed in typical elicitin members. According to the classification system developed for elicitins and related proteins (Jiang *et al*., 2006), PAR9 and PAR10, absent from the mycelium library, belonged to the clade ELL-1, and were renamed PARL1A and PARL1B, respectively. As a whole, elicitins and related proteins were underrepresented in the interaction library compared with the mycelium library (139 ESTs; Panabières *et al*., 2005). The abundant PAR5 and PAR6 were absent in the interaction library (Fig. 4). Comparison of *P. sojae* cDNA libraries (Qutob *et al*., 2003) and experimental results obtained using RNA isolated from infected leaves indicated that expression of class I elicitins (e.g. INF1 and PARA1) is repressed during early steps of compatible interactions, but increases at later stages (Kamoun *et al*., 1997; Colas *et al*., 2001). The present, contrasting data may reflect differences between root and leaf invasion.

'Cytoplasmic effectors' of *P. parasitica* included the two members of the R × LR family already described and three CRN-like proteins, displaying best matches with the *P. infestans* CRN5, CRN13 and CRN14, respectively (Win *et al.*, 2006). This effector family was originally described through the identification in *P. infestans* of *CRN1* and *CRN2* (crinkling and necrosis), two genes that are expressed during infection of the host tomato and that induce defence-related genes (Torto *et al.*, 2003).

We also identified sequences relevant to protein maturation, folding and secretion, which may participate in the secretion of effectors during infection and may potentially be indirectly involved in their activity. We assembled 97 ESTs into 30 contigs (Table S2), including various chaperones, heat-shock (*hsp*) proteins and other proteins required for proper folding and translocation of proteins (Gething & Sanbrook, 1992). Only 17 of these genes were found among 36 ESTs in the mycelium library, although differences in number of ESTs were rarely supported by statistical analyses (according to Audic & Claverie, 1997; Table S2). The chaperone GRP78/BiP was identified in one EST from the mycelium library and nine sequences in the interaction library, suggesting a differential expression ($0.005 < P < 0.004$). Similarly, a cDNA encoding a member of the *Hsp70* family (accession AAR21576; Shan & Hardham, 2004) was significantly upregulated during infection ($0.002 < P < 0.001$). Several *hsp* genes have been shown to be upregulated in germinating cysts of *P. infestans*, and some are induced during infection (Avrova *et al.*, 2003). The *H. parasitica GRP78/BiP* gene is also highly expressed during infection of *A. thaliana* (Bittner-Eddy *et al.*, 2003). *Hsp* proteins are considered as virulence determinants in bacterial, protozoan and yeast pathogens (Miller *et al.*, 1999; Gophna & Ron, 2003). Whether they play a role in *Phytophthora* pathogenicity has to be investigated.

## Other genes potentially related to pathogenicity

Potential pathogenicity factors included destructive enzymes and genes enabling the pathogen to evade or suppress plant defences. Among these, 61 ESTs of the interaction library, assembled into 27 cDNAs, encoded glycosyl hydrolases belonging to nine distinct classes (Henrissat, 1991), as well as a pectin lyase and a pectin methyl esterase (Table 1). A large majority (21/27) were absent from the mycelium library, but the diffrential representation between the two libraries was generally not supported by statistical analysis (not shown). Seventeen out of 27 were predicted to be secreted, using PSORT and SIGNALP programs, suggesting that these hydrolases could have a role in nutrition or growth at late stages of infection, and may function in virulence.

We also found 23 cDNAs with similarity to aspartyl (1), serine (7) and cysteine (7) proteases, and eight potential metalloproteases. A signal peptide was identified in six predicted proteins, corresponding to a cathepsin E-like protease, two cysteine proteases, two serine proteases, and a protein with similarity (43% positive, $E = 3e\text{-}16$) to Zn-dependent metalloproteases from insects. Interestingly, this protein belongs to the MEROPS peptidase subfamily M12A (astacin family), which is found in a variety of eukaryotes, but is absent from plants and yeast. One of the two cysteine proteases secreted also possesses a cysteine protease inhibitor domain (MEROPS family I29) in its N-terminus. It may aid in nutrition and growth, but may also participate in a general counterdefence strategy against tomato proteases possessing a possible dual function in virulence. Another cDNA was found with similarity to a member of the diverse family of Kazal-like serine protease inhibitors already identified in oomycetes, completing the arsenal of virulence factors of *Phytophthora* (Tian *et al.*, 2004; Torto-Alalibo *et al.*, 2005).

Central in the defence of plants against pathogen attack, reactive oxygen intermediates (ROIs) are associated with establishment of the hypersensitive response (Levine *et al.*, 1994). To survive, succeed the first penetration steps and further invade the tissues, the pathogen has to inactivate or remove the ROIs (Mayer *et al.*, 2001). Several sequences relevant to protection against ROIs were identified in the ESTs, including superoxide dismutase, thioredoxin peroxidases, glutaredoxin-related sequences, and glutathione *S*-transferases (Table 2). Because they can counteract toxic effects of the oxidative burst, they may contribute to pathogenesis. We also identified sequences potentially involved in efflux and detoxification, including putative cytochrome $P_{450}$ proteins, FAD-dependent monooxygenases, and 17 cDNAs matching ABC transporters, among which 14 were absent from the mycelium library (Table 2). Through their role in detoxification, they may contribute to the success of infection. Alternatively, they may participate in the secretion of toxins.

## Metabolic changes on infection deduced from EST representation

We used the ESTs to examine the *P. parasitica* metabolism during infection. Reconstructing the glycolytic pathway revealed special features. We identified seven distinct cDNAs displaying extensive matches with GA3PDH, including three sequences that were absent from the mycelium library. From our previous (Panabières *et al.*, 2005) and present analyses, at least 10 different genes potentially encode GA3PDH-related proteins in *P. parasitica*. They display the residues required for glycolytic activity (Sirover, 1999), encoding functional enzymes. GAPDH is now considered as a multifunctional enzyme that possesses numerous nonglycolytic activities, frequently caused by various cellular locations (Sirover, 1999), including resistance to oxidative stress (Grant *et al.*, 1999). In addition, its involvement in virulence has been demonstrated in several organisms (Pancholi & Chhatwal, 2003). The consequence of GAPDH diversity in the biology and pathogenicity of *Phytophthora* now needs to be investigated.

 

**Table 1** *Phytophthora parasitica* glycosyl hydrolases

| Contig/EST | Family | Function | Accession | Organism | *E* | Interaction* | Mycelium† | Secretion‡ | Homologues§ |
|---|---|---|---|---|---|---|---|---|---|
| i0030 | GH17 | Endo-1,3-beta-glucanase (endo1) | AF494013 | *P. infestans* | 6e-126 | 2 | 0 | Y | +++ |
| i0058 | GH5 | Cell 5 A endo-1,4-betaglucanase | ABG80554 | *P. ramorum* | 4e-126 | 2 | 0 | Y | –++ |
| i0103 | GH5 | Exo-1,3-beta-glucanase (exo3) | AAM18484 | *P. infestans* | 0 | 2 | 0 | Y | +++ |
| i0113 | GH5 | Endo-beta-1,6-galactanase | ZP_01462102 | *S. aurantiaca* | 3e-71 | 3 | 0 | Y | +++ |
| i0132 | GH3 | Glycoside hydrolase | YP_678877 | *C. hutchinsonii* | 2e-35 | 2 | 0 | Y | +++ |
| i0179 | GH26 | CEL4b mannanase | CAA90423 | *A. bisporus* | 2e-58 | 2 | 0 | Y | +++ |
| i0183 | GH30 | Glycoside hydrolase | ZP_01188247 | *H. orenii* | 3e-36 | 2 | 0 | Y | +++ |
| int-10f1 | GH31 | α-glucosidase II | XP_867560 | *C. familiaris* | 6e-40 | 1 | 0 | N | +++ |
| int-15e8 | | Pectin lyase | Q00374 | *C. gloeosporioides* | 1e-32 | 1 | 0 | Y | +++ |
| int-19h12 | GH28 | Polygalacturonase 2 | AAN36413 | *P. cinnamomi* | 1e-106 | 1 | 0 | Y | +++ |
| int-27b11 | GH5 | Cell 5 A endo-1,4-betaglucanase | ABL75349 | *P. ramorum* | 1e-113 | 1 | 0 | N | +++ |
| int-33g2 | GH5 | Endo-beta-1,4-glucanase | AAL83749 | *Paenibacillus* sp. | 4e-39 | 1 | 0 | N | +++ |
| int-34f8 | | Pectin methyl esterase | CAC29255 | *B. fuckeliana* | 1e-27 | 1 | 0 | Y | +++ |
| int-35f4 | GH17 | Endo-1,3-beta-glucanase (endo1) | AF494013 | *P. infestans* | 3e-58 | 1 | 0 | Y | +++ |
| int-36g8 | GH5 | Cell 5 A endo-1,4-betaglucanase | ABG91066 | *P. ramorum* | 8e-133 | 1 | 0 | N | +++ |
| int-3e9 | GH30 | *O*-glycosyl hydrolase | ZP_00886342 | *C. saccharolyticus* | 1e-46 | 1 | 0 | Y | +++ |
| int-40a5 | GH6 | Exocellobiohydrolase precursor | AF174362 | *P. rhizinflata* | 7e-18 | 1 | 0 | Y | +++ |
| int-4d1 | GH30 | Glycoside hydrolase | NP_623885 | *T. tengcongensis* | 7e-09 | 1 | 0 | N | +++ |
| int-8e10 | GH30 | β-glucosidase/xylosidase | AF352032 | *P. infestans* | 8e-36 | 1 | 0 | N | +++ |
| int-9h12 | GH30 | β-glucosidase/xylosidase | AF352032 | *P. infestans* | 1e-48 | 1 | 0 | Y | +++ |
| T-149-0075 | GH26 | CEL4b mannanase | CAA90423 | *A. bisporus* | 1e-22 | 2 | 3 | Y | +++ |
| T-149-0102 | GH5 | Exo-1,3-beta-glucanase (exo1) | AAM18483 | *P. infestans* | 0 | 10 | 14 | Y | +++ |
| T-149-0260 | GH19 | Acidic chitinase | AAN31509 | *P. infestans* | 1e-113 | 2 | 2 | Y | +++ |
| T-149-0410 | GH30 | β-glucosidase/xylosidase | AF352032 | *P. infestans* | 4e-127 | 3 | 4 | ? | +++ |
| T-149-0490 | GH19 | Acidic chitinase | AAN31509 | *P. infestans* | 1e-73 | 1 | 2 | Y | +++ |
| T-149-0493 | GH17 | Glycosyl hydrolase | ZP_01732735 | *F.* bacterium BAL38 | 2e-10 | 14 | 3 | Y | +++ |

*Abundance among 2989 ESTs.
†Abundance among 3568 ESTs.
‡See Materials and Methods.
§Presence of a homologue in other *Phytophthora* species. +++, present in *P. infestans*, *P. ramorum* and *P. sojae*. –++, absent in *P. infestans*.

**Table 2** *Phytophthora parasitica* sequences relevant to antioxidant defences and detoxication

| Contig | Putative function | Organism | Accession | *E* | Interaction* | Mycelium† |
|---|---|---|---|---|---|---|
| i0064 | Phospholipid hydroperoxide glutathione peroxidase | *P. sojae* | ABA29804 | 1e-110 | 3 | 0 |
| i0065 | Cytochrome $P_{450}$, putative | *A. thaliana* | AAG60111 | 3e-22 | 2 | 0 |
| i0100 | ATP-binding cassette transporter AtABCA1 | *A. thaliana* | AAK39643 | 1e-35 | 2 | 0 |
| i0109 | ATP-binding cassette transporter AtABCA1 | *A. thaliana* | AAK39643 | 4e-35 | 2 | 0 |
| i0182 | Nucleoredoxin | *D. rerio* | NP_001018431 | 3e-23 | 2 | 0 |
| int-10b8 | ATP-binding cassette, subfamily D | *C. familiaris* | XP_537064 | 5e-72 | 1 | 0 |
| int-10h6 | ABC transporter, putative | *A. thaliana* | AAC31858 | 3e-36 | 1 | 0 |
| int-11f4 | ATP-binding cassette, subfamily C | *S. purpuratus* | XP_788510 | 1e-05 | 1 | 0 |
| int-14d12 | Thioredoxin reductase | *R. norvegicus* | AAH85726 | 7e-67 | 1 | 0 |
| int-14g4 | FAD-dependent monooxygenase | *P. aeruginosa* | AAG08606 | 5e-18 | 1 | 0 |
| int-15e4 | Thioredoxin | *D. melanogaster* | AAF66635 | 2e-24 | 1 | 0 |
| int-16e8 | Glutaredoxin | *P. atlantica* | YP_663014 | 2e-34 | 1 | 0 |
| int-17f1 | Peroxidoxin | *L. major* | CAJ03825 | 8e-46 | 1 | 0 |
| int-18f7 | Cytochrome $P_{450}$, CYP94B2 | *G. max* | ABD97099 | 6e-13 | 1 | 0 |
| int-20e12 | Cytochrome $P_{450}$, CYP86C1 | *A. thaliana* | NP_173862 | 2e-18 | 1 | 0 |
| int-23e10 | ABC transporter AbcG1 | *D. discoideum* | AAL91485 | 2e-41 | 1 | 0 |
| int-24d1 | Glutaredoxin | *N. crassa* | XP_961585 | 4e-16 | 1 | 0 |
| int-26b10 | Glutathione *S*-transferase | *P. putida* | ZP_00898449 | 2e-09 | 1 | 0 |
| int-26e10 | ATP-binding cassette, subfamily C | *D. rerio* | NP_956883 | 1e-66 | 1 | 0 |
| int-27f10 | Thioredoxin | *C. annuum* | AAR83852 | 2e-19 | 1 | 0 |
| int-29e3 | Glutathione *S*-transferase | *A. aegypti* | EAT41547 | 9e-04 | 1 | 0 |
| int-32d3 | ABC transporter, putative | *A. thaliana* | AAF98206 | 1e-31 | 1 | 0 |
| int-33a1 | Thioredoxin peroxidase | *P. infestans* | AAN31487 | 7e-76 | 1 | 0 |
| int-33g11 | ABC transporter, putative | *O. sativa* | XP_450985 | 3e-28 | 1 | 0 |
| int-35b1 | ABC transporter, putative | *O. sativa* | XP_450985 | 7e-45 | 1 | 0 |
| int-37e12 | Glutathione *S*-transferase, theta class | *P. infestans* | CAK02792 | 3e-26 | 1 | 0 |
| int-37f10 | ATP-binding cassette, subfamily A | *D. rerio* | XP_693353 | 1e-05 | 1 | 0 |
| int-38a2 | ATP-binding cassette transporter AtABCA1 | *A. thaliana* | AAK39643 | 6e-12 | 1 | 0 |
| int-39a8 | Cytochrome $P_{450}$, CYP96A1 | *A. thaliana* | BAC42368 | 2e-32 | 1 | 0 |
| int-42d4 | Putative PDR-like ABC transporter | *O. sativa* | BAD53546 | 8e-38 | 1 | 0 |
| int-42f9 | ATP-binding cassette, subfamily B | *D. rerio* | XP_692515 | 4e-30 | 1 | 0 |
| int-6a4 | Thioredoxin | *Helicosporidium* | AAU93947 | 1e-13 | 1 | 0 |
| int-9f11 | Glutaredoxin | *P. atlantica* | YP_663014 | 3e-37 | 1 | 0 |
| t-149-0020 | ATP-binding cassette transporter AtABCA1 | *A. thaliana* | AAK39643 | 1e-82 | 1 | 4 |
| T-149-0109 | Glutathione reductase | *L. monocytogenes* | EAL07715 | 2e-56 | 1 | 2 |
| T-149-0110 | Glutathione *S*-transferase | *A. thaliana* | BAB11100 | 1e-23 | 3 | 4 |
| T-149-0146 | ABC transporter | *N. mobilis* | ZP_01126396 | 9e-105 | 1 | 1 |
| t-149-0309 | Putative MATE efflux family protein | *O. sativa* | XP_462988 | 7e-14 | 1 | 2 |
| T-149-0330 | Manganese superoxide dismutase | *P. nicotianae* | AAY57577 | 0 | 8 | 7 |
| t-149-0420 | ATP-binding cassette transporter AtABCA1 | *A. thaliana* | AAK39643 | 1e-61 | 1 | 3 |
| T-149-0448 | Thioredoxin-like | *D. pseudoobscura* | EAL29599 | 8e-19 | 1 | 2 |
| T-149-0522 | Glutaredoxin type I | *F. agrestis* | AAB92658 | 2e-17 | 2 | 1 |
| T-149-0563 | Glutathione synthetase | *L. esculentum* | AAB71231 | 1e-86 | 1 | 1 |
| T-149-0576 | Glutathione *S*-transferase | *O. tauri* | CAL53338 | 7e-60 | 3 | 1 |
| T-149-0711 | Cytochrome $P_{450}$, CYP94B3 | *A. thaliana* | AAU94404 | 5e-23 | 1 | 1 |
| T-149-0719 | Glutaredoxin-related protein | *Z. mobilis* | YP_163608 | 7e-26 | 1 | 1 |
| T-149-0750 | Peroxiredoxin | *H. sapiens* | NP_005800 | 6e-76 | 1 | 1 |
| T-149-0751 | Thioredoxin, putative | *T. gondii* | CAJ20392 | 4e-14 | 1 | 1 |

*Abundance among 2989 ESTs.
†Abundance among 3568 ESTs.

Differing from observations in most eukaryotes, we identified two enzymes using pyrophosphate as substrate instead of ATP. They are pyrophosphate-dependent phosphofructokinase (PPi-PFK) and pyruvate phosphate dikinase (PPDK). They replace ATP-dependent enzymes catalysing irreversible steps: ATP-dependent phosphofructokinase (ATP-PFK) and pyruvate kinase, respectively (Mertens, 1993). PPi-PFK and PPDK catalyse reversible reactions and may then act in glycolysis as well as gluconeogenesis. A hypothesis is that late in the infection, the pathogen faces a limitation in glucose, and

 

using PPi-dependent enzymes would improve the energy efficiency when the substrate level is limited (Mertens, 1993). Four genes encoding PPDK have been cloned in *P. cinnamomi* (Marshall *et al.*, 2001). Surprisingly, their expression pattern revealed a significant increase in the corresponding mRNA in nutrient-free medium, although the protein and enzyme activity levels remain unchanged (Marshall *et al.*, 2001). This observation led to the hypothesis that PPi can be used as an energy source in limiting conditions. Our present data reinforce this hypothesis.

The number of sequences related to the TCA cycle is low, and the entire pathway could not be reconstructed from our data. Yet five ESTs correspond to malate synthase, a key enzyme of the glyoxylate cycle, which bypasses the TCA cycle. Considering that several enzymes of the TCA cycle identified in our ESTs may also participate in the glyoxylate cycle, we may suppose that this metabolic pathway is active at this step of infection. This is not unexpected: accumulating reports indicate that the glyoxylate cycle is required for the growth of animal and plant pathogens during infection and is necessary for virulence (Lorenz & Fink, 2001, 2002; Idnurm & Howlett, 2002).

If the TCA cycle is not functional during the late phase of infection, we have to consider the fate of pyruvate, and characterize additional sources of ATP. The identification of pyruvate : ferredoxin oxidoreductase (PFOR) suggests that pyruvate can be converted to acetyl-CoA, which may subsequently be converted to acetate with ATP generation by acetyl-CoA synthase (ACS), represented by two ESTs. Finding three cDNAs encoding distinct lactate dehydrogenases suggests that, alternatively, pyruvate is converted to lactate. Last, the identification of several enzymes relevant to amino acid degradation, such as threonine dehydratase, associated to PFOR and ACS, suggests that amino acids may constitute a supplementary nutrient source used by *P. parasitica* in infected tissues.

## Experimental validation of *in silico* comparative analyses

Quantitative real-time RT–PCR was used to validate the *in silico* expression results, using cDNAs derived from *in vitro* growth of *P. parasitica* or from 4-d-infected tomato roots. A set of 16 genes (Table 3) was selected on the basis of significant differences in their representation among EST libraries, except for two sequences that could be used as constitutively expressed internal controls. A first control corresponded to ubiquitin-conjugating enzyme (Ubc), which was represented by three and two ESTs in each library, respectively, and which was previously shown to be constitutively expressed during tomato leaf invasion by *P. parasitica* (Yan & Liou, 2006). Another potential control was a gene encoding a superoxide dismutase, represented by eight and seven ESTs in the mycelium and interaction libraries, respectively. The genes encoding the glucose-regulated/BiP protein and a protein disulfide isomerase appeared to be repressed during invasion,

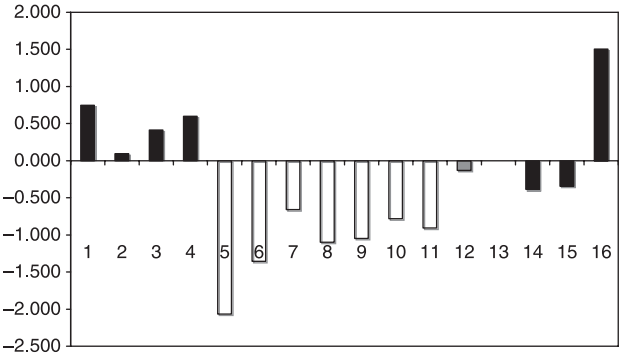


**Fig. 5** Real-time RT–PCR expression profiles of 16 *Phytophthora parasitica* genes (see Table S3) in *P. parasitica*-infected tomato roots 4 d after inoculation. Expression values are relative to those for vegetative mycelium. Black bars, genes with representation significantly higher in the interaction library; white bars, genes with representation significantly higher in the mycelium library. Grey bar, a sequence equally represented in both libraries.

compared with vegetative growth, whereas they were highly overrepresented in the interaction library (Fig. 5; Table S3). The two genes selected as constitutively expressed controls were transcribed at similar rates in the two situations, as expected from EST analysis. Lastly, 12 out of the 16 genes displayed differential expression between vegetative growth *in vitro* and tomato root invasion, as previously predicted from EST library comparisons (Fig. 4; Table S3). For example, the expression of ParA1 and PAR6 decreased dramatically, in total accordance with analysis of EST data sets. Therefore the experimental results supported *in silico* expression patterns for 14 out of the 16 candidate genes (87.5%).

## Concluding remarks

We report here the combination of histological and molecular approaches to exploring tomato root colonization by *P. parasitica*. Gaining insight into the mode of colonization of *P. parasitica* will help to develop new control strategies against the pathogen. The use of CLSM allowed the spatial and temporal analysis of infection on, around and within roots, and revealed details on all colonization steps.

ESTs described here help to describe the molecular events accompanying the necrotrophic stage of the *P. parasitica* infection cycle. With up to 80% of ESTs generated from the pathogen, the present report constitutes an important contribution to the identification of *Phytophthora* genes expressed during a compatible interaction, still allowing the identification of substantial host sequences that are expressed late in infection. The present work follows an EST project developed on a cDNA library from *in vitro*-grown mycelium. Merging the two data sets led to the generation of a collection of 3405 unigenes. The genome size of *P. parasitica* is 95.5 Mb (Shan & Hardham, 2004), similar to *P. sojae*, which possesses *c.* 19 000 genes (Tyler *et al.*, 2006). Thus we may consider that the two *P. parasitica*

**Table 3** Oligonucleotide primers used in real-time RT–PCR expression analysis of selected *Phytophthora parasitica* genes, and amplicon size

| Contig | Putative function | Organism | *E* | Amplicon size (bp) | Real-time RT–PCR forward and reverse primers |
|---|---|---|---|---|---|
| i0001 | Sodium ion/solute transporter | *O. lucimarinus* | 5e-34 | 134 | 5′-CTCACGACCATGTTGTCACC-3′<br>5′-ACTCCAATACCCTGCCACAC-3′ |
| i0060 | Phosphatidylinositol 3- and 4-kinase | *M. truncatula* | 1e-38 | 141 | 5′-GTTCACAAGATCGGCATCCT-3′<br>5′-CTTGTACGACGGCAGACAGA-3′ |
| i0092 | Secretory protein OPEL | *P. parasitica* | 1e-54 | 136 | 5′-CCGGAGGTTCAAGGTGACTA-3′<br>5′-ACATCGTCTTGGAGGTGGTC-3′ |
| i0166 | Succinate-semialdehyde dehydrogenase | *B. multivorans* | 6e-64 | 172 | 5′-ATGTCCGCAAGATCTCGTTC-3′<br>5′-AACTTTGACGCCATCAGTCC-3′ |
| T-149-0014 | Aquaporin 7 | *X. tropicalis* | 4e-26 | 168 | 5′-TCTGTACCGACCGATGTTCA-3′<br>5′-TTGTGCTGGTCCAGTAGTGC-3′ |
| T-149-0094 | Par5 | | | 103 | 5′-AGAACGTGCAGGCTACCAAC-3′<br>5′-CATCCAGGCTCGAAGTTGTC-3′ |
| T-149-0095 | Par6 | | | 183 | 5′-CCTCGGAATCAGGCTACAAC-3′<br>5′-AGGCGAGTTGGTACACGTTC-3′ |
| t-149-0097 | ParA1 | | | 188 | 5′-CAACAAGATCGTGACGCTGA-3′<br>5′-CGTACTTGGCACGAAGACAA-3′ |
| t-149-0117 | No significant hit | | | 149 | 5′-CTACCAAGACTTCGGGACGA-3′<br>5′-ATTCCGGTGAAAGACCACTG-3′ |
| t-149-0119 | Hypothetical protein | *P. troglodytes* | 3e-27 | 128 | 5′-ATACCGAGACTACGCCATGC-3′<br>5′-TGTAGTCGCACCTGTTCCAG-3′ |
| t-149-0168 | Delta-9 desaturase | *P. tricornutum* | 3e-39 | 157 | 5′-TACGCTATGTGCTCGACCTG-3′<br>5′-AACTTGTGGTGCCAGTTGTG-3′ |
| T-149-0330 | Superoxide dismutase | *P. nicotianae* | 0 | 164 | 5′-CCAGGCTTACGTGAACAACA-3′<br>5′-AGGTCATCCACGTCCAGAAG-3′ |
| T-149-0382 | Ubiquitin-conjugating enzyme (Ubc) | *P. infestans* | 2e-75 | 152 | 5′-CCACTTAGAGCACGCTAGGA-3′<br>5′-TACCGACTGTCCTTCGTTCA-3′ |
| T-149-0520 | Protein disulfide isomerase | *P. troglodytes* | 3e-105 | 106 | 5′-ATGGAAAGTTGACGCCTCTG-3′<br>5′-TTGTCGATCACACGCTTCTC-3′ |
| T-149-0543 | Glucose-regulated protein/BiP | *P. cinnamomi* | 0 | 125 | 5′-CTCGAACTTGCCCAGAAGAC-3′<br>5′-TTATCCCGACCAAGAAGTCG-3′ |
| T-149-0566 | Hypothetical protein | *A. clavatus* | 3e-15 | 116 | 5′-CTCGGTCTTCCTGCTCTTTG-3′<br>5′-TCTCCACGATGACGAAGATG-3′ |

EST libraries, with samplings of moderate size, theoretically allowed the identification of approx. 18% of *P. parasitica* genes.

Global transcriptional changes were hypothesized on the assumption that the number of ESTs reflects the level of expression of a gene in a given situation. We intended to validate this approach on 16 candidates using a quantitative RT–PCR (qPCR) strategy. In 14 of 16 cases, the qPCR data supported the expression pattern anticipated by EST comparisons. Thus comparative *in silico* analyses afford an opportunity to study the biology of the pathogen in colonized tissues, and the metabolic changes occurring during infection, towards exploring the nutritional basis of pathogenicity of *Phytophthora*.

## Acknowledgements

We thank Virginie Colas and Paul Venard for their contribution to the initial steps of this work and Philippe Montuquet for assistance in sequence handling. We are grateful to Mathieu Gourgues and Valérie Allasia for their help with q-RT–PCR, Eric Galiana for helpful discussions and Julie Hopkins for proofreading the manuscript. This work was funded by grants from INRA, Direction scientifique 'Plante et Produits du végétal' and Department 'Santé des Plantes et Environnement'.

## References

**Apweiler R, Attwood TK, Bairoch A *et al.* 2001.** The InterPro database, an integrated documentation resource for protein families, domains and functional sites. *Nucleic Acids Research* **29**: 37–40.

**Armstrong MR, Whisson SC, Pritchard L *et al.* 2005.** An ancestral oomycete locus contains late blight avirulence gene *Avr3a*, encoding a protein that is recognized in the host cytoplasm. *Proceedings of the National Academy of Sciences, USA* **102**: 7766–7771.

**Audic S, Claverie JM. 1997.** The significance of digital gene expression profiles. *Genome Research* **7**: 986–995.

**Avrova AO, Venter E, Birch PR, Whisson SC. 2003.** Profiling and quantifying differential gene transcription in *Phytophthora infestans* prior to and during the early stages of potato infection. *Fungal Genetics and Biology* **40**: 4–14.

**Benhamou N, Côté F. 1992.** Ultrastructure and cytochemistry of pectin and cellulose degradation in tobacco roots infected by *Phytophthora parasitica* var. *nicotianae. Phytopathology* **82**: 468–478.

**Beyer K, Jimenez Jimenez S, Randall TA, Lam S, Binder A, Boller T, Collinge M. 2002.** Characterization of *Phytophthora infestans* genes regulated during the interaction with potato. *Molecular Plant Pathology* **3**: 473–485.

**Bittner-Eddy PD, Allen RL, Rehmany AP, Birch PRJ, Beynon JL. 2003.** Use of suppression substractive hybridization to identify downy mildew genes expressed during infection of *Arabidopsis thaliana*. *Molecular Plant Pathology* **4**: 501–507.

**Bottin A, Larche L, Villalba F, Gaulin E, Esquerre-Tugayé MT, Rickauer M. 1999.** Green fluorescent protein (GFP) as gene expression reporter and vital marker for studying development and microbe–plant interaction in the tobacco pathogen *Phytophthora parasitica* var. *nicotianae. FEMS Microbiology Letters* **176**: 51–56.

**Brunner F, Rosahl S, Lee J, Rudd JJ, Geiler C, Kauppinen S, Rasmussen G, Scheel D, Nurnberger T. 2002.** Pep-13, a plant defense-inducing pathogen-associated pattern from *Phytophthora transglutaminases*. *The EMBO Journal* **21**: 6681–6688.

**Colas V, Lacourt I, Ricci P, Valenberghe-Masutti F, Venard P, Poupet A, Panabières F. 1998.** Diversity of virulence *in Phytophthora parasitica* on tobacco, as reflected by nuclear RFLPs. *Phytopathology* **88**: 205–212.

**Colas V, Conrod S, Venard P, Keller H, Ricci P, Panabières F. 2001.** Elicitin genes expressed in vitro by some tobacco isolates of *Phytophthora parasitica* are down-regulated during compatible interactions. *Molecular Plant–Microbe Interactions* **14**: 326–335.

**Erwin D, Ribeiro O. 1996.** *Phytophthora diseases worldwide*. St Paul, MN, USA: American Phytopathological Society.

**Fabritius AL, Judelson HS. 2003.** A mating-induced protein of *Phytophthora infestans* is a member of a family of elicitors with divergent structures and stage-specific patterns of expression. *Molecular Plant–Microbe Interactions* **16**: 926–935.

**Gaulin E, Jauneau A, Villalba F, Rickauer M, Esquerre-Tugaye MT, Bottin A. 2002.** The CBEL glycoprotein of *Phytophthora parasitica* var. *nicotianae* is involved in cell wall deposition and adhesion to cellulosic substrates. *Journal of Cell Science* **115**: 4565–4575.

**Gething MJ, Sanbrook J. 1992.** Protein folding in the cell. *Nature* **355**: 33–45.

**Gijzen M, Nurnberger T. 2006.** Nep1-like proteins from plant pathogens: recruitment and diversification of the NPP1 domain across taxa. *Phytochemistry* **67**: 1800–1807.

**Gophna U, Ron EZ. 2003.** Virulence and the heat shock response. *International Journal of Medical Microbiology* **292**: 453–461.

**Grant CM, Quinn KA, Dawes IW. 1999.** Differential protein *S*-thiolation of glyceraldehyde-3-phosphate dehydrogenase isoenzymes influences sensitivity to oxidative stress. *Molecular and Cellular Biology* **19**: 2650–2656.

**Grenville-Briggs LJ, Avrova AO, Bruce CR, Williams A, Whisson SC, Birch PR, van West P. 2005.** Elevated amino acid biosynthesis in *Phytophthora infestans* during appressorium formation and potato infection. *Fungal Genetics and Biology* **42**: 244–256.

**Hanchey P, Wheeler H. 1971.** Pathological changes in ultrastructure: tobacco roots infected with *Phytophthora parasitica* var. *nicotianae. Phytopathology* **61**: 33–39.

**Henrissat B. 1991.** A classification of glycosyl hydrolases based on amino-acid sequence similarities. *Biochemical Journal* **280**: 309–316.

**Huitema E, Torto TA, Styer A, Kamoun S. 2003.** Combined ESTs from plant–microbe interactions: using GC counting to determine the species of origin. *Methods in Molecular Biology* **236**: 79–84.

**Idnurm A, Howlett BJ. 2002.** Isocitrate lyase is essential for pathogenicity of the fungus *Leptosphaeria maculans* to canola (*Brassica napus*) *Eukaryotic Cell* **1**: 719–724.

**Jiang RH, Tyler BM, Whisson SC, Hardham AR, Govers F. 2006.** Ancient origin of elicitin gene clusters in *Phytophthora* genomes. *Molecular Biology and Evolution* **23**: 338–351.

**Judelson HS. 1993.** Intermolecular ligation mediates efficient cotransformation in *Phytophthora infestans*. *Molecular and General Genetics* **239**: 241–250.

**Kamoun S. 2006.** A catalogue of the effector secretome of plant pathogenic oomycetes. *Annual Review of Phytopathology* **44**: 41–60.

**Kamoun S, van West P, de Jong AJ, de Groot KE, Vleeshouwers VG, Govers F. 1997.** A gene encoding a protein elicitor of *Phytophthora infestans* is down-regulated during infection of potato. *Molecular Plant–Microbe Interactions* **10**: 13–20.

**Laroche-Raynal M, Aspart L, Delseny M, Penon P. 1984.** Characterization of radish mRNA at three developmental stages. *Plant Science* **35**: 139–146.

**Levine A, Tenhaken R, Dixon R, Lamb C. 1994.** $H_2O_2$ from the oxidative burst orchestrates the plant hypersensitive disease resistance response. *Cell* **79**: 583–593.

**Lorenz MC, Fink GR. 2001.** The glyoxylate cycle is required for fungal virulence. *Nature* **412**: 83–86.

**Lorenz MC, Fink GR. 2002.** Life and death in a macrophage: role of the glyoxylate cycle in virulence. *Eukaryotic Cell* **1**: 657–662.

**Marshall JS, Ashton AR, Govers F, Hardham AR. 2001.** Isolation and characterization of four genes encoding pyruvate, phosphate dikinase in the oomycete plant pathogen *Phytophthora cinnamomi*. *Current Genetics* **40**: 73–81.

**Mayer AM, Staples RC, Gil-ad NL. 2001.** Mechanisms of survival of

necrotrophic fungal plant pathogens in hosts expressing the hypersensitive response. *Phytochemistry* **58**: 33–41.

**Meissner R, Jacobson Y, Melamed S, Levyyatuv S, Shalev G, Ashri A, Elkind Y, Levy AA. 1997.** A new model system for tomato genetics. *Plant Journal* **12**: 1465–1472.

**Mertens E. 1993.** ATP versus pyrophosphate: glycolysis revisited in parasitic protists. *Parasitology Today* **9**: 122–126.

**Miller CMD, Smith NC, Johnson AM. 1999.** Cytokines, nitric oxyde, heat shock proteins and virulence in toxoplasma. *Parasitology Today* **15**: 418–422.

**Moy P, Qutob D, Chapman BP, Atkinson I, Gijzen M. 2004.** Patterns of gene expression upon infection of soybean plants by *Phytophthora sojae*. *Molecular Plant–Microbe Interactions* **17**: 1051–1062.

**Nakai K, Kanehisa M. 1992.** A knowledge base for predicting protein localization sites in eukaryotic cells. *Genomics* **14**: 897–911.

**Panabières F, Ansalem J, Galiana E, Le Berre J-Y. 2005.** Gene identification in the oomycete pathogen *Phytophthora parasitica* during *in vitro* vegetative growth through expressed sequence tags (ESTs). *Fungal Genetics and Biology* **42**: 611–623.

**Pancholi V, Chhatwal GS. 2003.** Housekeeping enzymes as virulence factors for pathogens. *International Journal of Medical Microbiology* **293**: 391–401.

**Pieterse CMJ, Riach MBR, Bleker T, van der Berg-Velthuis GCM, Govers F. 1993.** Isolation of putative pathogenicity genes of the potato late blight fungus *Phytophthora infestans* by differential hybridization of a genomic library. *Physiological and Molecular Plant Pathology* **43**: 69–79.

**Qutob D, Hraber PT, Sobral BW, Gijzen M. 2000.** Comparative analysis of expressed sequences in *Phytopthora sojae*. *Plant Physiology* **123**: 243–253.

**Qutob D, Huitema E, Gijzen M, Kamoun S. 2003.** Variation in structure and activity among elicitins from *Phytophthora sojae*. *Molecular Plant Pathology* **4**: 119–124.

**Qutob D, Kamoun S, Gijzen M. 2002.** Expression of a *Phytophthora Sojae* necrosis-inducing protein occurs during transition from biotrophy to necrotrophy. *Plant Journal* **32**: 361–373.

**Randall TA, Dwyer RA, Huitema E *et al.* 2005.** Large-scale gene discovery in the oomycete *Phytophthora infestans* reveals likely components of phytopathogenicity shared with true fungi. *Molecular Plant–Microbe Interactions* **18**: 229–243.

**Rawlings ND, Barrett AJ. 1999.** MEROPS: the peptidase database. *Nucleic Acids Research* **27**: 325–331.

**Rehmany AP, Gordon A, Rose LE, Allen RL, Armstrong MR, Whisson SC, Kamoun S, Tyler BM, Birch PR, Beynon JL. 2005.** Differential recognition of highly divergent downy mildew avirulence gene alleles by *RPP1* resistance genes from two Arabidopsis lines. *Plant Cell* **17**: 1839–1850.

**Shan W, Hardham AR. 2004.** Construction of a bacterial artificial chromosome library, determination of genome size, and characterization of an *Hsp70* gene family in *Phytophthora nicotianae*. *Fungal Genetics and Biology* **41**: 369–380.

**Shan W, Cao M, Leung D, Tyler BM. 2004a.** The *Avr1b* locus of *Phytophthora sojae* encodes an elicitor and a regulator required for avirulence on soybean plants carrying resistance gene *Rps1b*. *Molecular Plant–Microbe Interactions* **17**: 394–403.

**Shan W, Marshall JS, Hardham AR. 2004b.** Gene expression in germinated cysts of *Phytophthora nicotianae*. *Molecular Plant Pathology* **5**: 317–330.

**Sirover MA. 1999.** New insights into an old protein: the functional diversity of mammalian glyceraldehyde-3-phosphate dehydrogenase. *Biochemica et Biophysica Acta* **1432**: 159–184.

**Skalamera D, Wasson AP, Hardham AR. 2004.** Genes expressed in zoospores of *Phytophthora nicotianae*. *Molecular Genetics and Genomics* **270**: 549–557.

**Soanes DM, Skinner W, Keon J, Hargreaves J, Talbot NJ. 2002.** Genomics of phytopathogenic fungi and the development of bioinformatic resources. *Molecular Plant–Microbe Interactions* **15**: 421–427.

**Tian M, Huitema E, Da Cunha L, Torto-Alalibo T, Kamoun S. 2004.** A Kazal-like extracellular serine protease inhibitor from *Phytophthora infestans* targets the tomato pathogenesis-related protease P69B. *The Journal of Biological Chemistry* **279**: 26370–26377.

**Torto TA, Li S, Styer A, Huitema E, Testa A, Gow NA, van West P, Kamoun S. 2003.** EST mining and functional expression assays identify extracellular effector proteins from the plant pathogen *Phytophthora*. *Genome Research* **13**: 1675–1685.

**Torto-Alalibo T, Tian M, Gajendran K, Waugh ME, van West P, Kamoun S. 2005.** Expressed sequence tags from the oomycete fish pathogen *Saprolegnia parasitica* reveal putative virulence factors. *BMC Microbiology* **5**: 46.

**Torto-Alalibo TA, Tripathy S, Smith BM *et al.* 2007.** Expressed sequence tags from *Phytophthora sojae* reveal genes specific to development and infection. *Molecular Plant–Microbe Interactions* **20**: 781–793.

**Tripathy S, Pandey VN, Fang B, Salas F, Tyler BM. 2006.** VMD: a community annotation database for oomycetes and microbial genomes. *Nucleic Acids Research* **34**: D379–D381.

**Tyler BM, Tripathy S, Zhang X *et al.* 2006.** *Phytophthora* genome sequences uncover evolutionary origins and mechanisms of pathogenesis. *Science* **313**: 1261–1266.

**Villalba Mateos F, Rickauer M, Esquerre-Tugaye MT. 1997.** Cloning and characterization of a cDNA encoding an elicitor of *Phytophthora parasitica* var. *nicotianae* that shows cellulose-binding and lectin-like activities. *Molecular Plant–Microbe Interactions* **10**: 1045–1053.

**Win J, Kanneganti TD, Torto-Alalibo T, Kamoun S. 2006.** Computational and comparative analyses of 150 full-length cDNA sequences from the oomycete plant pathogen *Phytophthora infestans*. *Fungal Genetics and Biology* **43**: 20–33.

**Yan HZ, Liou RF. 2006.** Selection of internal control genes for real-time quantitative RT–PCR assays in the oomycete plant pathogen *Phytophthora parasitica*. *Fungal Genetics and Biology* **43**: 430–438.

## Supplementary Material

The following supplementary material is available for this article online:

**Fig. S1** Schematic structure of the transformation vector pTefGHNH containing the selectable marker gene (*nptII*) and the reporter gene encoding green fluorescent protein under control of the *Phytophthora parasitica* promoter (*PpTef1prom*) of the translation elongation vector (see text).

**Table S1** *Phytophthora parasitica* sequences identified only in the interaction library

**Table S2** *Phytophthora parasitica* sequences relevant to protein folding and maturation

**Table S3** Expression of selected *Phytophthora parasitica* genes deduced from their relative representation in EST libraries and from real-time RT–PCR experiments

This material is available as part of the online article from http://www.blackwell-synergy.com/doi/abs/10.1111/j.1469-8137.02269.x
(This link will take you to the article abstract.)

Please note: Blackwell Publishing are not responsible for the content or functionality of any supplementary materials supplied by the authors. Any queries (other than about missing material) should be directed to the *New Phytologist* Central Office.

 